Electric Power Systems Research 151 (2017) 283–295

Contents lists available at ScienceDirect

Electric Power Systems Research

journal homepage: www.elsevier.com/locate/epsr

A demand power factor-based approach for finding the maximum loading point

Mahdi Pourakbari-Kasmaei[a,*], Javier Contreras[b], José Roberto Sanches Mantovani[a]

[a] Department of Electrical Engineering, Power System Planning Lab, Universidade Estadual Paulista (UNESP), Ilha Solteira, SP, Brazil
[b] E.T.S. de Ingenieros Industriales, University of Castilla-La Mancha, 13071 Ciudad Real, Spain

ARTICLE INFO

Article history:
Received 14 February 2017
Received in revised form 29 May 2017
Accepted 31 May 2017
Available online 10 June 2017

Keywords:
Demand power factor
Flexible loading pattern
Maximum loading point
Optimal power flow

ABSTRACT

This paper presents a demand power factor-based approach (DPFA) for finding the maximum loading point (MLP) of a power system using the optimal power flow (OPF). In almost all the presented models in the literature two major drawbacks are obvious: (1) the active and reactive power demands increase equally, constantly, or at the same rate, while in the real world, this hardly ever occurs, and (2) the lack of consideration or misinterpretation of the demand power factor (DPF). This paper addresses the existing drawbacks by proposing a model based on a desired DPF, a threshold predefined by the independent system operator (ISO) that each consumer must maintain to prevent a surcharge. In the proposed DPFA, the active and reactive demands may increase differently resulting in: (1) providing a flexible loading pattern to find the best possible MLP, (2) keeping the desired DPFs at all load buses, and (3) improving the computational efficiency. To verify the DPFA, which is solvable via commercial solvers, several cases such as IEEE 14-, 30-, modified 30-, and 118-bus systems, and a large-scale 2338-bus system are conducted. Results confirm the potential, effectiveness, and superiority of the DPFA compared to the models in the literature.

1. Introduction

From an operational standpoint, the maximum loading point (MLP), is the maximum load that a power system can serve without violating generation, transmission, and operation constraints [1]. MLP-based analysis is an efficient way to evaluate a power system in a steady state and provides a more practical sense of a security margin for system operators [2].

In deregulated environments, power systems work under stress and, as a consequence, a heavily loaded power system has a higher tendency toward instability [3]. Testing a power system under the MLP condition can identify the critical buses, branches, or the weakest areas, which play an essential role in power system operation. The application of the MLP is not only limited to operation-based problems, but also provides useful information for planning-, scheduling-, and market-based problems, e.g. transmission expansion planning, tie-line planning, FACTS placement, unit commitment, distributed generation sizing, etc. [4–6]. In the technical literature, one of the most important issues to consider is the maximum demand of a system, especially for planning problems [7–9].

In order to find the MLP of a system, various mathematical models and optimization techniques, such as classical, heuristic-based, and hybrid methods have been proposed [10]. A simple method to find the MLP is the use of conventional power flow tools to gradually increase the demands until convergence no longer exists [11]. The drawback of this method is not only the need for manual intervention but also the uncertainty of knowing where the limits are. Although finding the MLP using power flow tools is well established problem and some of the existing drawbacks have been addressed [12,13], in today's competitive world precise information is the keystone of decision-making based problems, and this cannot be obtained via a simple economic dispatch or conventional power flow tools. Another obstacle in this area of research is that the enhancements to power flow-based approaches cannot be properly applied to OPF-based approaches, which consider more practical network constraints [14]. In recent years, in order to find the appropriate MLP, OPF-based models have been widely used, which play an important role in the operating-based, decision-making-based, and market-driven problems [7,15–17]. Note that the OPF-based model has been presented in Refs. [18,19] as an extension of the power flow-based model in Refs. [20,21].

* Corresponding author at: Av. Brasil 056, UNESP—Campus de Ilha Solteira, Departamento de Engenharia Elétrica, Sala 52, Ilha Solteira, 15385000 São Paulo, Brazil.
E-mail addresses: mahdi.pourakbari@ieee.org, mant@dee.feis.unesp.br (M. Pourakbari-Kasmaei), Javier.Contreras@uclm.es (J. Contreras).

http://dx.doi.org/10.1016/j.epsr.2017.05.042
0378-7796/

Nomenclature

Sets

Ω_b	Set of buses, $\{1, 2, \ldots, N_b\}$
Ω_{PQ}	Set of PQ buses, $\{1, 2, \ldots, N_{PQ}\}$, $\Omega_{PQ} \subseteq \Omega_b$
Ω_{PV}	Set of PV buses, $\{1, 2, \ldots, N_{PV}\}$, $\Omega_{PV} \subseteq \Omega_b$
Ω_g	Set of generating units, $\{1, 2, \ldots, N_g\}$, $\Omega_g \subseteq \Omega_b$
Ω_l	Set of transmission elements, $\{1, 2, \ldots, N_l\}$

Indices

i, j	Bus indices; $i, j \in \Omega_b$
l	Transmission element indices; $l \in \Omega_l$

Variables and functions

a_{ij}^l, φ_{ij}^l	Adjustable magnitude and phase shifting of transformer taps at line l, corridor ij
fl_{ij}^l	Power flow of line l, corridor ij
F_T	Objective function
$pf_{D_i}^v$	Adjustable demand power factor at each PQ bus i
P_{g_i}	Active power generation of unit i
$P_{D_i}^{new}$	Active power demand under the MLP condition at bus i
$P_{D_i}^v$	Adjustable active power demand at bus i
p_{ij}^l, p_{ji}^l	Direct and reverse active power injections of line l, corridor ij
q_{ij}^l, q_{ji}^l	Direct and reverse reactive power injections of line l, corridor ij
Q_{g_i}	Reactive power generation of unit i
$Q_{D_i}^{new}$	Reactive power demand under the MLP condition at bus i
$Q_{D_i}^v$	Adjustable reactive power demand at bus i
$S_{D_i}^v$	Adjustable apparent power demand at PQ bus i
tp_{ij}^l	Transformer tap of line l, corridor ij
V_i	Voltage magnitude at bus i
λ	Common loading factor for all demand buses
λ_i	Loading factor of demand bus i
δ_i	Phase angle at bus i
θ_{ij}^l	Voltage angle difference between bus i and j, $\theta_{ij}^l = \delta_i - \delta_j$, along with line l
ρ_i	Reactive demand ratio at bus i

Parameters

$b_{ij}^{l,ch}$	Charging susceptance of line l, corridor ij
$b_i^{b,sh}$	Shunt susceptance of bus i (ʊ)
b_{ij}^l	Susceptance (ʊ) of line l, corridor ij
$\overline{fl_{ij}^l}$	Maximum power flow of line l, corridor ij
g_{ij}^l	Conductance (Ω) of line l, corridor ij
$g_i^{b,sh}$	Shunt conductance of bus i (Ω)
$P_{D_i}^0$	Initial active power demand at bus i
$\underline{P_{g_i}}$,$\overline{P_{g_i}}$	Minimum and maximum active power generation limits of unit i
$Q_{D_i}^0$	Initial reactive power demand at bus i
$\underline{Q_{g_i}}$,$\overline{Q_{g_i}}$	Minimum and maximum reactive power generation limits of unit i
$\underline{tp_{ij}^l}$, $\overline{tp_{ij}^l}$	Minimum and maximum limits of transformer tap of line l, corridor ij
$\underline{V_i}$, $\overline{V_i}$	Minimum and maximum voltage magnitude limits of bus i
ΔP_{D_i}	Pre-specified rate of increase of active demand at bus i
ΔQ_{D_i}	Pre-specified rate of increase of reactive demand at bus i
$\cos\phi_i$	Constant demand power factor at bus i
η_i	Predefined multipliers to designate the rate of loading at bus i

Until now, to the best of our knowledge, in most OPF-based works the reactive power demand increases with a predefined and usually incorrect relationship with the active power demand in order to find the MLP [22,23]. In general, for such mathematical formulations, the demands increase until either the limited induced bifurcation (LIB) or saddle-node bifurcation (SNB) limits are reached [24]. This does not mean that the system is below the MLP, which is a physical limit, it shows the divergence of the power flow calculation, which is a mathematical failure [25]. In order to consider the advantages and shortcomings of the existing models and their evolution to be more applicable, we classify the mathematical models in three groups, such as common loading factor-, different loading rate-, and individual loading factor-based models. These models are shown in detail as follows.

1.1. Common loading factor-based model

In some works, to find the MLP of a system using an OPF-based model, the loading factors at all buses are considered equal, this is called the common loading factor (CLF), which is a widely-used model in power system studies [15,26–28]. The general OPF-based model presented in these works is shown in Eqs. (1)–(8).

$$\max \lambda \tag{1}$$

subject to:

$$P_{g_i} - P_{D_i}^{new} - g_i^{b,sh} V_i^2 - \sum_{ij \in \Omega_l} p_{ij}^l - \sum_{ji \in \Omega_l} p_{ji}^l = 0; \forall i \in \Omega_b \tag{2}$$

$$Q_{g_i} - Q_{D_i}^{new} + b_i^{b,sh} V_i^2 - \sum_{ij \in \Omega_l} q_{ij}^l - \sum_{ji \in \Omega_l} q_{ji}^l = 0; \forall i \in \Omega_b \tag{3}$$

$$|f_{ij}^l(V, \delta, tp)| \le \overline{f_{ij}^l}; \forall ij, l \in \Omega_l \tag{4}$$

$$\underline{V_i} \le V_i \le \overline{V_i}; \forall i \in \Omega_b \tag{5}$$

$$\underline{P_{g_i}} \le P_{g_i} \le \overline{P_{g_i}}; \forall i \in \Omega_g \tag{6}$$

$$\underline{Q_{g_i}} \le Q_{g_i} \le \overline{Q_{g_i}}; \forall i \in \Omega_g \tag{7}$$

$$\underline{tp_{ij}^l} \le |tp_{ij}^l| \le \overline{tp_{ij}^l}; \forall ij, l \in \Omega_l \tag{8}$$

where the active and reactive power demands under the MLP condition in Eqs. (2) and (3) are defined in Eqs. (9) and (10), respectively. The direct and reverse active and reactive power flows are defined in Section 2 of Ref. [14].

$$P_{D_i}^{new} = (1 + \lambda) \cdot P_{D_i}^0 \tag{9}$$

$$Q_{D_i}^{new} = (1 + \lambda) \cdot Q_{D_i}^0 \tag{10}$$

In this formulation, for all PQ buses, the one that reaches its maximum loading capacity before the others defines the MLP of the system. Therefore, the loading factor of the system is the loading factor corresponding to the bus which has the lowest value. This

loading factor follows the min–max rule, (Eq. (11)). However, it prevents the system from finding an acceptable MLP.

$$\min_{\lambda}\{\max_{i\in\Omega_{PQ}}\lambda\} \tag{11}$$

Although this commonly used model is fast enough to be used in operating-based problems, however, it has the following drawbacks.

D1) As the MLP is equal to the lowest loading factor obtained among all PQ buses, it adversely affects further decisions to be made based on it.

D2) The active and reactive power demands increase at the same rate, while in a real power system they may change at different rates.

D3) If a PQ bus is initially without load, based on Eqs. (9) and (10), still remains without load, limiting system loadability.

D4) The lack of consideration of a controllable demand power factor (DPF), which plays an important role in practice.

1.2. Different loading rate-based model

The different loading rate-based model (DLR), in which the active and reactive demands may increase with different loading rates is aimed at addressing some drawbacks of the CLF model. The first representation of this model, DLR-1, has been proposed in Ref. [18] and later in Ref. [2], as a more efficient model than the CLF, and has been used to identify weak buses. Its mathematical formulation is the same as Eqs. (1)–(10), except for constraints (9) and (10) that become Eqs. (12) and (13), respectively. The loading factors for different bus types are considered in Eq. (14). See that in Ref. [18], instead of maximizing the loading factor, its inverse, $1/\lambda$, is minimized, which may result in computational inefficiency for buses with zero loadability.

$$P_{D_i}^{new}=P_{D_i}^{0}+\lambda\eta_i\cos\phi_i \tag{12}$$

$$Q_{D_i}^{new}=Q_{D_i}^{0}+\lambda\eta_i\sin\phi_i \tag{13}$$

$$\begin{cases}\lambda\geq 0,\forall i\in\Omega_{PQ}\\ \lambda=0,\forall i\in\Omega_{PV}\end{cases} \tag{14}$$

As it can be seen in the model, a constant DPF has been considered. On the other hand, since the desired DPF usually lies within the interval [0.85, 0.98], where $\sin\phi$ is always lower than $\cos\phi$, $\sin\phi<\cos\phi$, and, consequently, the reactive demand quantity increases reasonably compared with the active power demand.

Almost the same model has been proposed in Ref. [29], where Eq. (13) becomes Eq. (15). This yields a new drawback in which the active and reactive power demands increase equally, which hardly ever occurs in a real system.

$$Q_{D_i}^{new}=Q_{D_i}^{0}+\lambda\eta_i\cos\phi_i \tag{15}$$

Another representation of this model, DLR-2, has been proposed in [30], by converting Eqs. (9) and (10) into Eqs. (16) and (17), respectively. In this model, the active power demand is adjustable, $P_{D_i}^{\nu}$, while the reactive power is a function of active demand and a predefined DPF. One of the benefits of this model is the degree of freedom of the active power demand, $P_{D_i}^{\nu}$, however, it uses a constant loading factor, λ, may negatively affect the result.

$$P_{D_i}^{new}=P_{D_i}^{0}+\lambda P_{D_i}^{\nu} \tag{16}$$

$$Q_{D_i}^{new}=Q_{D_i}^{0}+\lambda P_{D_i}^{\nu}\cos\phi_i \tag{17}$$

Although in all the aforementioned models the active and reactive demands do not increase at the same rate, they increase constantly or equally, while in a real system this hardly ever occurs. Therefore, these models fail in addressing D2, as expected. Another drawback of these models is that the DPF is not controllable and, therefore, there is no guarantee of keeping the desired DPF under a new loading condition. For instance, assume that the desired DPF is chosen to be greater than or equal to 0.9 and the initial active and reactive demands are 1 MW and 0.8 MVAr, respectively, then, the initial DPF yields $\cos\phi\approx 0.78087$. On the other hand, because there is no control on the DPF under the MLP condition, the control variable can be adjusted so that the best MLP is obtained. Therefore, one possibility could be to adjust all these control variables, λ, $P_{D_i}^{\nu}$, and η_i, to 1. Hence, for the model presented in Refs. [2,18], DLR-1, the new active and reactive demands are 1.9 MW and 1.23589 MVAr, respectively, and with these new demands, a new DPF is calculated with $\cos\phi_i\approx 0.83826$. For the models presented in Refs. [29,30], DLR-2, the calculated DPFs are $\cos\phi_i\approx 0.74524$ and $\cos\phi_i\approx 0.7250$, respectively. As it can be seen, all the aforementioned models fail in satisfying the desired DPF, and consequently, the fourth drawback, D4, still remains.

A more flexible model has been presented in Refs. [31,32], in which the active and reactive power demands at each PQ bus could increase according to their own pre-specified active and reactive increase rates, respectively, as shown in Eqs. (18) and (19).

$$P_{D_i}^{new}=P_{D_i}^{0}+\lambda^2\Delta P_{D_i} \tag{18}$$

$$Q_{D_i}^{new}=Q_{D_i}^{0}+\lambda^2\Delta Q_{D_i} \tag{19}$$

The shortcomings of this model are: (1) in order to find the best pre-specified rates of each bus, a trial and error method is necessary; therefore, in large-scale systems finding the best pre-specified rates for each bus is a complicated task and it may require an additional process, and (2) the constant loading factor may negatively affect the solution results. In Refs. [31,32], for the sake of simplicity, the rates are considered equal. Thereby, the active and reactive power demands increase equally, which is considered as a significant shortcoming in real system operations.

However, the main drawback of the models presented in Refs. [2,18], and Refs. [29–32] is their weakness in properly loading the PQ buses with initial negative reactive demands, while the reactive demand at such buses may become even positive under the MLP condition. In Ref. [33], in order to address this drawback, a simplified model based on Ref. [30] has been used; however, the reactive demand in all PQ buses have been fixed to the initial demand, which is not acceptable in practice.

1.3. Individual loading factor-based model

In this model, to have a more flexible model, each PQ bus has its corresponding individual loading factor (ILF), λ_i. To obtain this model, the objective function, (1), and constraints (9) and (10) are converted into Eqs. (20)–(22), respectively [34].

$$\max\sum_{i\in\Omega_{PQ}}\lambda_i \tag{20}$$

$$P_{D_i}^{new}=(1+\lambda_i)\cdot P_{D_i}^{0} \tag{21}$$

$$Q_{D_i}^{new}=(1+\lambda_i)\cdot Q_{D_i}^{0} \tag{22}$$

Although the aforementioned model addresses the first drawback of the CLF model, D1, the other drawbacks, D2–D4, still remain. On the other hand, besides nonlinearity, in a large-scale system, the number of variables corresponding to the loading factors may decrease the computational efficiency making it difficult to find an optimal solution.

The other common drawback of the three presented models (CLF, DLF, and ILF) is the use of a loading factor, λ or λ_i, for active

and reactive power demands that has to be maximized. This inadequate definition may result in an unacceptable MLP because, in some buses, the reactive demand may reach its limit before the active demand reaches its own and, based on this loading factor, the model may find an unacceptable MLP. In other words, these models aim at maximizing the joint loading factor and not the MLP. Consequently, there is no guarantee of finding the maximum possible loading point.

This paper aims at addressing the aforementioned shortcomings by proposing a demand power factor-based approach (DPFA). The main contributions of the proposed DPFA are as follows.

1) Capability of increasing active and reactive power demands with different loading rates, producing more realistic results by providing flexible loading rates.
2) Capability of loading all PQ buses (initially under load or no-load conditions).
3) 3Considering the minimum acceptable demand power factor, which is a threshold predefined by the ISO. This determines the maximum reactive power that each consumer can demand without a surcharge. This DPF is a function of the adjustable active and reactive demands and consequently, can be easily controlled.

To verify the proposed DPFA and show its effectiveness, several case studies such as IEEE 14-, 30-, and 118-bus systems, a modified 30-bus system (30-bus-M), and a large-scale 2383-bus Polish system are conducted.

The rest of this paper is organized as follows. Section 2 shows the proposed DPFA model. Case studies and results are presented in section 3. Section 4 presents the concluding remarks and prospects for future works.

2. Demand power factor-based model

The demand power factor (DPF) is a predefined threshold that plays an important role in a power system to control the consumers active-reactive demand ratio. This DPF, which is a value defined by the ISO, highly depends on the system topology and loading conditions, such as different active and reactive load levels, occurrence of different contingencies, different reactive support devices, different reserve conditions, etc. This factor considers the peculiar nature of reactive power by evaluating the system under the aforementioned conditions to satisfy the minimum/maximum voltage limits. Therefore, the two main components used to determine this factor are: (1) zero-VAR interchange (if a multi-area system is considered), and (2) minimum/maximum voltage limits [35]. In this paper, in addition to considering the DPF, all the other existing drawbacks are addressed. To obtain the proposed demand power factor-based approach (DPFA), constraints (2) and (3) are converted into Eqs. (24) and (25), respectively, in model (1)–(10), and technical constraints (26)–(28) are also taken into account.

$$\max F_T = \sum_{i \in \Omega_{PQ}} S^{\nu}_{D_i} \; or \sum_{i \in \Omega_{PQ}} P^{\nu}_{D_i} \tag{23}$$

s.t. Constraints (4)–(8)

$$P_{g_i} - P^{\nu}_{D_i} - g^{b,sh}_i V_i^2 - \sum_{ij \in \Omega_l} p^l_{ij} - \sum_{ji \in \Omega_l} p^l_{ji} = 0; \forall i \in \Omega_b \tag{24}$$

$$Q_{g_i} - Q^{\nu}_{D_i} + b^{b,sh}_i V_i^2 - \sum_{ij \in \Omega_l} q^l_{ij} - \sum_{ji \in \Omega_l} q^l_{ji} = 0; \forall i \in \Omega_b \tag{25}$$

$$\begin{cases} P^{\nu}_{D_i} \geq P^0_{D_i}; if P^0_{D_i} \geq 0, \forall i \in \Omega_{PQ} \\ P^{\nu}_{D_i} = P^0_{D_i}; if P^0_{D_i} < 0, \forall i \in \Omega_{PQ} \end{cases} \tag{26}$$

$$\begin{cases} Q^{\nu}_{D_i} \geq Q^0_{D_i}; if Q^0_{D_i} \geq 0, \forall i \in \Omega_{PQ} \\ Q^{\nu}_{D_i} \leq Q^0_{D_i}; if Q^0_{D_i} < 0, \forall i \in \Omega_{PQ} \end{cases} \tag{27}$$

$$|Q^{\nu}_{D_i}| \leq \overline{Q^{\nu}_{D_i}}(pf^{\nu}_{D_i}, P^{\nu}_{D_i}); \forall i \in \Omega_{PQ} \tag{28}$$

In Eq. (23), the objective function is either the active power demand or the apparent power demand, which are maximized. In practice, the active power is usually maximized. The apparent power demand is defined below [36].

$$S^{\nu}_{D_i} = \sqrt{(P^{\nu}_{D_i})^2 + (Q^{\nu}_{D_i})^2}; \forall i \in \Omega_{PQ} \tag{29}$$

By defining the adjustable active and reactive demands in Eqs. (24) and (25), respectively, the three first drawbacks of the CLF model, D1–D3, are addressed. Unlike the models presented, in this model, the objective is not to maximize a factor corresponding to the active and/or reactive power demands, namely the loading factor; therefore, the proposed model is neither limited by the minmax rule nor by maximizing the loading factor. This model enhances the degree of freedom of such problems in which the active and reactive power demands may increase at different rates; accordingly, the second drawback, D2, is addressed. Constraints (26) and (27) guarantee that the active and reactive demands are non-decreasing, respectively. Constraint (26) implies that a PQ bus can be loaded if its initial active load is greater than or equal to zero in order to obtain the MLP, and the new demand must be greater than or equal to its initial active load under the MLP condition. Sometimes the active demand in a PQ bus is negative, which represents a supplier, and, in this study, remains constant. Constraint (27) implies that if the initial reactive demand in a PQ bus is inductive, $Q_D \geq 0$, or capacitive, $Q_D < 0$, under the MLP condition, it must become more inductive or capacitive, respectively. These two constraints not only guarantee the non-decreasing nature of active and reactive demands but also address the third drawback, D3, by providing the capability of loading all the PQ buses without considering their initial loading conditions. In practice, the quantity of the reactive power that can be demanded by a consumer has its own flexible upper limit, which is a function of the active demand and the demand power factor, as shown in Eq. (28). This flexible upper limit can be calculated as follows.

From the technical literature, the reactive power demand is a fraction of the active power demand, as shown in Eq. (30).

$$Q^{\nu}_{D_i} = \rho P^{\nu}_{D_i}; \forall i \in \Omega_{PQ} \tag{30}$$

On the other hand, each system has its own desired DPF, predefined by the ISO, depending on its topology and operational conditions, as shown in Eq. (31).

$$pf^{\nu}_{D_i} = \frac{P^{\nu}_{D_i}}{S^{\nu}_{D_i}}; \forall i \in \Omega_{PQ} \tag{31}$$

From Eqs. (29) and (31), the following relationship among active power, reactive power, and DPF is obtained, (Eq. (32)).

$$Q^{\nu}_{D_i} = P^{\nu}_{D_i} \cdot \sqrt{\left(\frac{1}{(pf^{\nu}_{D_i})^2} - 1\right)}; \forall i \in \Omega_{PQ} \tag{32}$$

By comparing Eq. (32) with Eq. (30), the reactive demand ratio (RDR), ρ_i, is defined in Eq. (33).

$$\rho_i = \sqrt{\left(\frac{1}{(pf^{\nu}_{D_i})^2} - 1\right)}; \forall i \in \Omega_{PQ} \tag{33}$$

Since the DPF is lower than or equal to 1, the maximum possible RDR occurs at the minimum possible DPF, $\underline{pf_{D_i}^v}$, in Eq. (33), therefore:

$$\overline{\rho_i} = \sqrt{\left(\frac{1}{\left(\underline{pf_{D_i}^v}\right)^2} - 1\right)}; \forall i \in \Omega_{PQ} \tag{34}$$

By placing this maximum ratio in Eq. (30), the maximum possible reactive power demand is:

$$\overline{Q_{D_i}^v} = \overline{\rho_i} P_{D_i}^v; \forall i \in \Omega_{PQ} \tag{35}$$

Consequently, if, for example, the minimum possible DPF in a system is 0.9 or 0.95, $\overline{Q_{D_i}^v}$ is achieved by setting the RDR to 0.4843 or 0.3287, respectively. According to Eq. (39), there is an inverse relationship between the DPF and the RDR, e.g., increasing the DPF toward 1 results in a reactive demand ratio (RDR) approaching zero, $\bar{\rho}_i = 0$, and, due to Eq. (40) this means that the consumers cannot demand reactive power. This is not acceptable in real power systems as consumers' loads are hardly ever purely resistive. Therefore, the higher the power factor, the lower the RDR, and, in contrast, the lower the power factor, the higher the RDR. Adjusting the DPF to a small value, on the one hand, may provide a higher degree of freedom for the consumers demanding reactive power but, on the other hand, it may negatively affect the operation and the benefits on the generation and delivery (transmission and distribution) sides. Once the DPF is determined by the ISO, the power plant and delivery system (transmission and distribution) owners can make a cost-benefit analysis taking into account this desired DPF. Consequently, if a consumer pulls excess current due to the low power factor, this consumer is wasting the generator's capacity and thus it cuts down the producers' ability to make a profit by selling power to other customers. The same happens on the delivery side; transmission lines and transformers are also capable of handling a limited amount of current and, requesting beyond this limit, results in heat and, consequently, decreases their potential in carrying current. To avoid such negative effects, a limit is defined for demanding reactive power to control the operating conditions by managing the reactive demands. Note that the acceptable range for the maximum reactive demand lies between 15% and 50% of the active demand, corresponding to power factors between 0.989 and 0.894, respectively, where demanding more reactive power than the predefined percentage results in a surcharge for the consumers. Consequently, this controllable DPF is considered as a remedy to the fourth drawback mentioned in the CLF model, D4, which makes our model even more applicable.

The direct and indirect active and reactive power flows are defined in Eqs. (36)–(39).

$$p_{ij}^l = (a_{ij}^l V_i)^2 g_{ij}^l - (a_{ij}^l V_i) V_j [g_{ij}^l \cos(\theta_{ij}^l + \varphi_{ij}^l) + b_{ij}^l \sin(\theta_{ij}^l + \varphi_{ij}^l)] \tag{36}$$

$$p_{ji}^l = g_{ij}^l V_j^2 - (a_{ij}^l V_i) V_j [g_{ij}^l \cos(\theta_{ij}^l + \varphi_{ij}^l) - b_{ij}^l \sin(\theta_{ij}^l + \varphi_{ij}^l)] \tag{37}$$

$$q_{ij}^l = -(a_{ij}^l V_i)^2 (b_{ij}^l + \frac{b_{ij}^{l,ch}}{2}) - (a_{ij}^l V_i) V_j [g_{ij}^l \cos(\theta_{ij}^l + \varphi_{ij}^l) - b_{ij}^l \sin(\theta_{ij}^l + \varphi_{ij}^l)] \tag{38}$$

$$q_{ji}^l = -(b_{ij}^l + \frac{b_{ij}^{l,ch}}{2}) V_j^2 + (a_{ij}^l V_i) V_j [g_{ij}^l \cos(\theta_{ij}^l + \varphi_{ij}^l) + b_{ij}^l \sin(\theta_{ij}^l + \varphi_{ij}^l)] \tag{39}$$

where transformer phase shifting, φ_{ij}^l, is neglected.

3. Case studies and results

Results from several case studies are presented in this section. First, we consider the IEEE 14-bus system under different conditions to highlight the properties of our proposed demand power factor-based approach. Then, three commonly used case studies such as IEEE 30-, modified 30- (30-bus-M), 57- and 118-bus systems are used to compare the results and show the superiority of the proposed DPFA. Finally, the proposed DPFA is applied to a large-scale power system such as the 2383-bus Polish system to show its potential in finding the MLP in big systems. To obtain a more practical result, the active power demand is maximized. The total reactive power demand values reported in the tables are the sum of the absolute values of the reactive power demands, $\sum_{i \in \Omega_b} |Q_{D_i}^v|$. It is worth mentioning that the main reasons for using DPF = 0.90 and 0.95 are: (1) showing the importance of determining an appropriate DPF by the ISO, (2) showing the impacts of DPF in finding the MLPs; the higher the DPF, the more restricted the system becomes in requesting reactive power.

The proposed model has been implemented on a personal computer with two processors at 2.67 GHz and 3 GB of RAM under AMPL [37] using KNITRO 7 [38]. In this paper, the interior point method, also known as the barrier method, which is one of the most effective methods in KNITRO, is used to solve the MLP problem.

3.1. Case 1: IEEE 14-bus system

The IEEE 14-bus system contains 9 PQ buses, 5 generation units, and 20 transmission lines [39]. Initially, the total active and reactive loads are 259 MW and 81.3 MVar, respectively. This system is tested under three different configurations: (C1) normal, (C2) considering line flow limits, and (C3) considering line outages and line flow limits. These tests are used to reveal the advantages and disadvantages of the proposed DPFA as well as comparisons with commonly used models. For this test system, the model presented in Ref. [30] fails in finding the MLP. In C2, the power flows of lines 1–2, 1–5, and 7–9 are limited to 110, 50, and 30 MW, respectively. In C3, an outage occurs in transmission line 1–2 and the power flow limits in transmission lines 1–5 and 7–9 are the same as for C2. To take into account the effects of FACTS devices on the solutions obtained by different models, the third condition, C3, is considered under different situations such as: (*i*) having static VAr compensator devices (SVC) and line charging susceptance (LCS), (*ii*) only having LCS, (*iii*) only having SVC, and (*iv*) having no FACTS devices.

Tables 1–3 show the optimal results obtained by the CLF, DLR-1, ILF, and the proposed DPFA models under three aforementioned configurations. The DLR-1 model obtains the worst result for all the three configurations. In this model, the capacitive reactive demand in bus 4 decreases, which is an important shortcoming. The ILF model under the three aforementioned configurations shows the best performance. However, the proposed DPFA allocates the loads appropriately among the consumers, and, consequently, provides a higher degree of freedom, obtaining a better solution. Under the normal configuration, C1, the total active loads obtained by the proposed model with DPF = 0.90 and DPF = 0.95 are 735.37 MW and 734.98, which, compared to the ILF model with 509.52 MW, show improvements of 44.33% and 44.23%, respectively. Considering the configurations with more limitations, C2 and C3, reveal that the proposed model highly depends on the system configuration as expected, and, if the configuration changes, the allocating patterns may change as well, and this flexibility helps in finding the best possible MLP, while the other models, based on their predefined allocating patterns, are not flexible. This can be seen in bus 7 which, under C1 configuration (Table 1), for all the models, is not loaded. However, under the C2 and C3 configurations (Tables 2 and 3, respectively), the DPFA provides different loading patterns corresponding to different system configurations. Meanwhile, the other models are not capable of providing such adaptive loading patterns and this bus still remains under its initial loading condition. Results

Table 1
Active and reactive demands at initial and MLPs under normal configuration—IEEE 14-bus system.

Bus #	Initial		CLF		DLR-1		ILF		DPFA			
	P_D	Q_D	P_D^{new}	Q_D^{new}	P_D^{new}	Q_D^{new}	P_D^{new}	Q_D^{new}	DPF = 0.90		DPF = 0.95	
									P_D^{new}	Q_D^{new}	P_D^{new}	Q_D^{new}
4	47.80	−3.90	108.24	−8.83	67.01	−2.33	47.80	−3.90	211.79	−71.61	194.55	−63.95
5	7.60	1.60	17.21	3.62	26.47	5.57	199.12	41.92	312.01	1.60	300.53	1.60
7	0.00	0.00	0.00	0.00	0.00	0.00	0.00	0.00	0.00	0.00	0.00	0.00
9	29.50	16.60	66.80	37.59	46.30	26.06	29.50	16.60	34.27	16.6	50.50	16.60
10	9.00	5.80	20.38	13.13	25.20	16.24	9.00	5.80	11.98	5.80	17.64	5.80
11	3.50	1.80	7.92	4.08	20.64	10.62	53.09	27.30	3.72	1.80	5.48	1.80
12	6.10	1.60	13.81	3.62	24.75	6.49	15.51	4.07	6.10	1.60	6.32	1.60
13	13.50	5.80	30.57	13.13	31.21	13.41	13.50	5.80	13.50	5.80	17.65	5.80
14	14.90	5.00	33.74	11.32	33.18	11.13	14.90	5.00	14.90	5.00	15.21	5.00
Non-PQ	127.10	39.20	127.10	39.20	127.10	39.20	127.10	39.20	127.10	39.20	127.10	39.20
Total	259.00	81.30	425.77	134.52	401.86	131.05	509.52	149.59	735.37	149.01	734.98	141.35

Table 2
Active and reactive demands at initial and MLPs considering line flow limits— IEEE 14-bus system.

Bus #	CLF		DLR-1		ILF		DPFA			
	P_D^{new}	Q_D^{new}	P_D^{new}	Q_D^{new}	P_D^{new}	Q_D^{new}	DPF = 0.90		DPF = 0.95	
							P_D^{new}	Q_D^{new}	P_D^{new}	Q_D^{new}
4	85.84	−7.00	59.93	−2.91	47.80	−3.90	260.27	−14.16	193.29	−3.90
5	13.65	2.87	19.51	4.11	90.27	19.00	7.60	3.68	7.60	2.50
7	0.00	0.00	0.00	0.00	0.00	0.00	43.74	10.72	79.00	12.24
9	52.98	29.81	40.11	22.57	29.50	16.60	34.28	16.60	50.50	16.60
10	16.16	10.42	19.23	12.39	9.00	5.80	11.98	5.80	17.64	5.80
11	6.28	3.23	14.32	7.37	63.26	32.54	3.72	1.80	5.48	1.80
12	10.95	2.87	17.88	4.69	6.10	1.60	6.10	2.96	6.10	2.00
13	24.24	10.42	24.68	10.60	13.50	5.80	13.50	6.54	17.65	5.80
14	26.76	8.98	26.44	8.87	14.90	5.00	14.90	5.00	15.21	5.00
Non-PQ	127.10	39.20	127.10	39.20	127.10	39.20	127.10	39.20	127.10	39.20
Total	363.96	114.80	349.20	112.71	401.43	129.44	523.19	106.46	519.56	94.84

Table 3
Active and reactive demands at initial and MLPs considering line outages and flow limits— IEEE 14-bus system.

Bus #	CLF		DLR-1		ILF		DPFA			
	P_D^{new}	Q_D^{new}	P_D^{new}	Q_D^{new}	P_D^{new}	Q_D^{new}	DPF = 0.90		DPF = 0.95	
							P_D^{new}	Q_D^{new}	P_D^{new}	Q_D^{new}
4	85.40	−6.97	59.78	−2.92	47.80	−3.90	74.91	−29.41	47.80	−15.71
5	13.58	2.86	19.36	4.08	67.32	14.17	141.36	1.60	106.54	1.60
7	0.00	0.00	0.00	0.00	0.00	0.00	56.37	2.26	89.09	0.00
9	52.71	29.66	39.98	22.50	29.50	16.60	34.28	16.6	50.50	16.60
10	16.08	10.36	19.10	12.31	9.00	5.80	11.98	5.80	17.64	5.80
11	6.25	3.22	14.19	7.30	64.73	33.29	3.72	1.80	5.48	1.80
12	10.90	2.86	17.73	4.65	6.10	1.60	6.10	1.60	6.10	1.60
13	24.12	10.36	24.54	10.54	13.50	5.80	13.50	5.80	17.65	5.80
14	26.62	8.93	26.30	8.82	14.90	5.00	14.90	5.00	15.21	5.00
Non-PQ	127.10	39.20	127.10	39.20	127.10	39.20	127.10	39.20	127.10	39.20
Total	362.76	114.42	348.08	112.32	379.95	125.36	484.22	109.07	483.11	93.11

show that the MLP obtained by the proposed DPFA with DPF = 0.95 is more restricted than the model with DPF = 0.90, compared to the UFL model, improving by 44.25%, 29.43%, and 27.15% under the first (C1), second (C2), and third (C3) configurations.

Fig. 1 presents the demand power factor obtained by the proposed DPFA in bus 4 under different system configurations, while the demand power factor obtained by different approaches in bus 10 is depicted in Fig. 2. From Fig. 1, it is observed that the demand power factor in the DPFA is not fixed to the predefined PDF value. However, this predefined value is used to define the maximum reactive power of a consumer, this being the minimum demand power factor. Fig. 2 also shows that even in the critical buses in which all the models are not capable of adjusting or even keeping the initial DPFs, while the DPFA adjusts the demands in such a way that the minimum DPF is satisfied.

Table 4 presents the results of different approaches such as security constrained genetic algorithm (SCGA) [2], particle swarm optimization (PSO) [40], hybrid PSO (HPSO) [40], differential evolution [33], hybrid DE and PSO (DEPSO) [33], multiagent particle swarm optimization (MAPSO) [41], multiagent-based hybrid particle swarm optimization (MAHPSO) [41], the CLF model presented in Refs. [26–28], the DLR-1 model in Refs. [2,18], the DLR-2 model in Ref. [30], the ILF model in Ref. [34], and the proposed DPFA with two demand power factors, 0.90 and 0.95. The CPU times of these methods are shown in Table 5.

Considering Table 4 for the IEEE 14-bus system, the worst result has been obtained by the SCGA, with 360.05 MW, that needs more CPU time, about 438 times, compared with the DPFA (DPF = 0.90), which has obtained the best solution, with 735.37 MW, as seen in Table 5. It can be seen that the DLR-2 model fails in

Table 4
Comparing the active (MW) and reactive (MVAr) demands of different approaches at MLP.

Methods		14-bus		30-bus		30-bus-M		57-bus		118-bus		2383-bus	
		P_D^{new}	Q_D^{new}	P_D^{new}	Q_D^{new}	P_D^{new}	Q_D^{new}	P_D^{new}	Q_D^{new}	P_D^{new}	Q_D^{new}	P_D^{new}	Q_D^{new}
PSO [40]		–	–	–	–	260.10	107.20	1403.90	336.40	5644.30	1439.00	–	–
HPSO [40]		–	–	–	–	260.35	107.20	1406.20	336.40	5644.50	1439.00	–	–
MAPSO [41]		–	–	–	–	260.81	107.20	–	–	5644.90	1439.00	–	–
MAHPSO [41]		–	–	–	–	260.81	107.20	–	–	5645.00	1439.00	–	–
DE [33]		–	–	–	–	267.09	107.20	–	–	5662.12	1439.00	–	–
DEPSO [33]		–	–	–	–	269.74	107.20	–	–	5701.60	1439.00	–	–
SCGA [2]		360.05	113.55	357.39	160.91	–	–	1448.63	399.13	4739.25	1620.175	–	–
CLF		425.77	134. 52	398.24	180.07	327.11	185.18	1290.53	348.99	6828.57	2385.63	27,917.29	9096.39
DLR-1		401.86	131.05	371.26	164.31	326.30	230.59	1265.30	341.75	6675.91	2360.20	27,997.20	9026.64
DLR-2		NC[a]	NC	367.48	201.87	205.18	121.58	1250.80	336.25	NC	NC	23,451.79	8033.45
ILF		509.52	149.59	420.92	187.71	326.34	167.03	1250.80	336.40	9354.91	3218.41	28,096.83	12,039.32
DPFA	DPF = 0.90	735.37	149.01	424.14	136.63	329.96	117.66	1933.62	352.63	9839.39	1604.58	29,142.98	8830.40
	DPF = 0.95	734.98	141.35	422.84	127.92	328.57	109.52	NC	NC	9835.24	1602.43	29,106.85	8668.24

[a] NC states that the model does not converge.

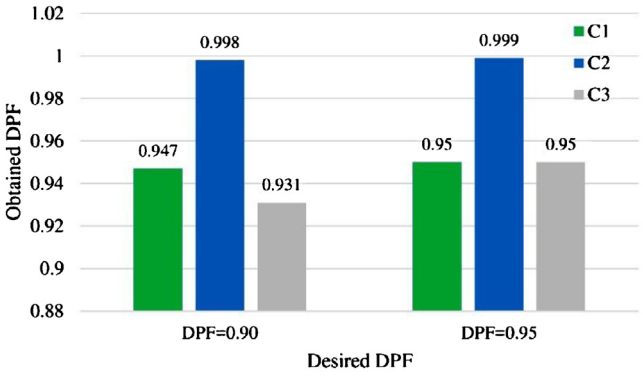

Fig. 1. Demand power factor at bus 4 using DPFA under different configurations—IEEE 14-bus system.

finding a solution. On the other hand, according to Table 5, the CLF, DLR-1, and DPFA models (DPF = 0.90) are the fastest with CPU times of 0.016 s, 0.019 s, and 0.020 s, respectively; however, the MLP obtained by the DPFA is much better than the other ones.

Reactive support devices are considered as one of the most efficient devices in power systems, especially under critical conditions. Table 6 shows the results of different approaches in finding the MLP of the 14-bus system under critical condition C3. As it can be seen from this table, FACTS devices do not significantly affect the MLPs of these models. This is because the reactive powers are mainly provided to the consumers by the generators and not by the reactive support devices. However, these reactive support devices are necessary to maintain the voltage magnitude of a bus at a specified value [42]. To show such effects, the voltage profile of different approaches in finding MLP under two situations: with FACTS devices (considering SVC and LCS) and without FACTS devices, as depicted in Fig. 3.

The voltage profiles of CLF, DLR-1, ILF, and DPFA are presented in Fig. 3 in subfigures a–d, respectively. Considering the voltage profile of the different approaches with and without FACTS devices shows that the voltage magnitude in most buses has decreased so that, in some buses, it reaches the critical operating point. The voltage profiles of the CLF, DLR-1, and ILF approaches show that without FACTS, there are at least three buses with a voltage magnitude below 0.98 p.u. Some voltage magnitudes hit the lower limit (bus 14 in CLF and bus 11 in ILF) or are close to the lower limit (bus 14 in DLR-1). However, the voltage profile in subfigure d shows that the proposed model, even for the case with a lower degree of freedom (DPF = 0.95), has the best potential in keeping the voltage profile at a safer point in which only the voltage at bus 14 is lower than 1.00 (0.995).

3.2. Case 2: IEEE 30-bus and 30-bus-M systems

These systems contain 24 PQ buses, 6 generation units, and 41 transmission lines. Data of the IEEE 30-bus and 30-bus-M systems

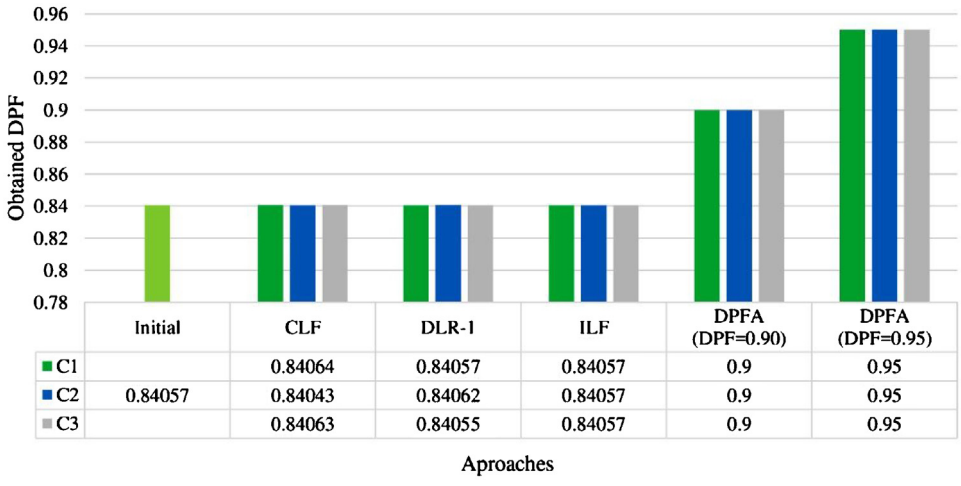

Fig. 2. Demand power factor at bus 10 using different approaches and under different configurations—IEEE 14-bus system.

Table 5
Comparison of CPU time (s) for different approaches.

Methods		14-bus	30-bus	30-bus-M	57-bus	118-bus	2383-bus
PSO [40]		–	–	61.36	67.23	69.91	–
HPSO [40]		–	–	39.80	8.10	51.15	–
MAPSO [41]		–	–	34.336	–	39.215	–
MAHPSO [41]		–	–	13.720	–	24.378	–
DE [33]		–	–	15.45	–	23.42	–
DEPSO [33]		–	–	13.51	–	22.82	–
SCGA [2]		39.48	78.24	–	148.76	327.56	–
CLF		0.016	0.042	0.068	0.097	0.947	24.128
DLR-1		0.019	0.048	0.031	0.132	0.835	24.389
DLR-2		NC	0.190	0.177	0.279	NC	191.711
ILF		0.038	0.043	0.039	0.096	0.448	75.987
DPFA	DPF = 0.90	0.090	0.060	0.046	0.093	0.312	6.902
	DPF = 0.95	0.020	0.056	0.054	NC	0.271	7.424

Table 6
Effects of FACTS devices on MLPs of different approaches— 14-bus, C3.

Situations	CLF	DLR-1	ILF	DPFA	
				DPF = 0.90	DPF = 0.95
With SVC and LCS	362.76	348.08	379.95	484.22	483.11
With LCS	362.62	348.11	387.17	484.17	482.99
With SVC	362.59	347.78	379.92	484.19	483.06
No FACTS	362.01	347.44	391.21	484.14	482.92

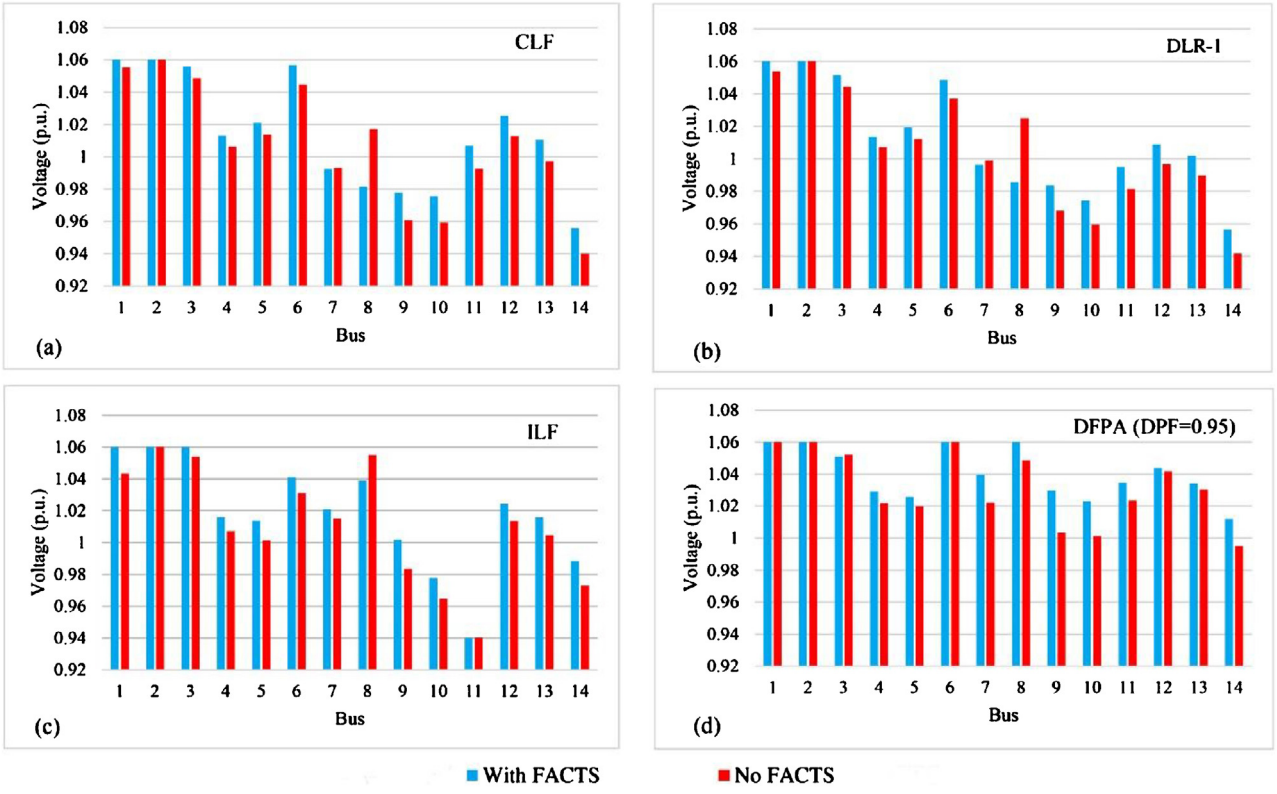

Fig. 3. Voltage profile of different approaches with and without considering FACTS devices—14-bus, C3.

can be found in Refs. [39,33], respectively. The initial active and reactive demands of IEEE 30-bus are 283.4 MW and 126.2 MVar while the 30-bus-M system has 189.2 MW and 107.2 MVar of active and reactive loads, respectively.

From Table 4, the ILF and SCGA models are the best and worst in finding the MLP of the IEEE 30-bus system, except for the DPFA, with 420.92 MW and 357.39 MW, respectively. The DPFA obtains higher MLPs, 424.14 MW for the case of DPF = 0.90, and 422.84 MW for the case of DPF = 0.95, showing the highest efficiency among all the approaches presented in this table. For this system, the same as in the IEEE 14-bus system, the SCGA has the lowest computational efficiency with 78.24 s CPU time, while the DPFA with DPF = 0.90 requires only 0.060 s, yet the SCGA cannot find an acceptable MLP.

In the literature, to find the best MLP of the 30-bus-M system, several heuristic-based approaches have been presented. In all

Table 7
Active (MW) and Reactive (MVar) Demands of Buses for Different Approaches at MLP— 30-bus-M System.

Bus	Initial demands		DEPSO [33]		CLF		DLR-1		DLR-2		ILF		DPFA			
	P_D	Q_D	P_D^{New}	Q_D^{New}	P_D^{New}	Q_D^{New}	P_D^{New}	Q_D^{New}	P_D^{New}	Q_D^{New}	P_D^{New}	Q_D^{New}	DPF = 0.90		DPF = 0.95	
													P_D^{New}	Q_D^{New}	P_D^{New}	Q_D^{New}
1	0	0	0	0	0	0	0	0	0	0	0	0	0	0	0	0
2	21.70	12.70	21.70	12.70	21.70	12.70	21.70	12.70	21.70	12.70	21.70	12.70	21.70	12.70	21.70	12.70
3	2.40	1.20	15.00	1.20	4.415	2.21	10.00	5.00	2.56	1.35	89.12	44.56	46.43	1.20	7.62	1.20
4	7.60	1.60	12.00	1.60	13.979	2.94	15.92	3.35	8.08	2.03	7.60	1.60	14.52	1.60	7.60	1.60
5	0	0	11.75	0	0	0	0	0	0.49	0.44	0	0	21.58	10.45	7.06	2.32
6	0	0	6.59	0	0	0	0	0	0.54	0.49	0	0	0	0	0	0
7	22.80	10.90	22.81	10.90	41.938	20.05	30.47	14.57	30.08	17.45	22.80	10.90	22.80	10.90	33.16	10.90
8	30.00	30.00	30.43	30.00	55.182	55.18	36.01	36.01	30.17	30.16	30.00	30.00	61.94	30.00	91.27	30.00
9	0	0	0.08	0	0	0	0	0	0.30	0.27	0	0	0	0	0	0
10	5.80	2.00	6.19	2.00	10.669	3.68	13.84	4.77	6.35	2.49	5.80	2.00	5.80	2.00	6.08	2.00
11	0	0	9.06	0	0	0	0	0	0.46	0.42	0	0	0	0	0	0
12	11.20	7.50	19.77	7.50	20.601	13.79	18.26	12.23	11.50	7.77	11.20	7.50	15.49	7.50	22.82	7.50
13	0	0	0	0	0	0	0	0	0	0	0	0	0	0	0	0
14	6.20	1.60	6.20	1.60	11.404	2.94	14.43	3.72	6.47	1.84	6.20	1.60	6.20	1.60	6.20	1.60
15	8.20	2.50	20.87	2.50	15.083	4.60	16.33	4.98	8.76	3.00	8.20	2.50	8.20	2.50	8.20	2.50
16	3.50	1.80	4.07	1.80	6.438	3.31	11.06	5.69	3.81	2.08	3.50	1.80	3.72	1.80	5.48	1.80
17	9.00	5.80	9.00	5.80	16.554	10.67	16.14	10.40	9.34	6.10	9.00	5.80	11.98	5.80	17.64	5.80
18	3.20	0.90	4.60	0.90	5.886	1.65	11.38	3.20	3.55	1.21	3.20	0.9	3.20	0.90	3.20	0.90
19	9.50	3.40	9.51	3.40	17.474	6.25	17.50	6.26	9.98	3.83	9.50	3.40	9.50	3.40	10.34	3.40
20	2.20	0.70	2.24	0.70	4.047	1.29	10.30	3.28	2.68	1.13	45.06	14.34	2.20	0.70	2.20	0.70
21	17.50	11.2	23.81	11.2	32.189	20.60	24.66	15.78	18.09	11.73	17.50	11.20	23.13	11.20	34.07	11.20
22	0	0	0	0	0	0	0	0	0	0	0	0	0	0	0	0
23	3.20	1.60	3.20	1.60	3.2	1.60	3.20	1.6	3.20	1.60	3.20	1.60	3.20	1.60	3.20	1.60
24	8.70	6.70	10.46	6.70	16.003	12.32	15.43	11.89	9.19	7.14	8.70	6.70	13.83	6.70	20.38	6.70
25	0	0	0.58	0	0	0	0	0	0.29	0.26	0	0	6.40	0	0	0
26	3.50	2.30	5.19	2.30	6.438	4.23	10.60	6.97	3.69	2.47	3.50	2.30	4.75	2.30	7.00	2.30
27	0	0	0	0	0	0	0	0	0	0	0	0	0	0	0	0
28	0	0	0.44	0	0	0	0	0	0.51	0.45	0	0	10.39	0	0	0
29	2.40	0.90	2.41	0.90	4.414	1.65	10.36	3.88	2.60	1.08	9.96	3.74	2.40	0.90	2.74	0.90
30	10.60	1.90	11.78	1.90	19.497	3.49	18.96	3.40	10.80	2.08	10.60	1.90	10.60	1.90	10.60	1.90

these models, only the active demands have increased and the reactive power demands are at their initial loading conditions. For this system, the best and the worst MLPs (except for the DPFA) belong to the CLF, with 327.11 MW, and the DLR-2, with 201.87 MW. Results show that the proposed DPFA, for the case with more restrictions (DPF = 0.95), obtains a higher MLP than the CLF model, about 2.23 MW, with a faster convergence, 25.93% higher.

Table 7 presents the active and reactive demands of the 30-bus-M system for different approaches to find the MLP. Among the heuristic-based algorithms presented in Table 4, only the maximum allowable loads of the DEPSO model have been reported in the literature. Results confirm that, by using the DPFA, even the buses that are initially under no-load conditions can be loaded if necessary, such as bus 28 in the case with DPF = 0.90, while the CLF, that obtains the best MLP among the approaches in the literature, is not capable of loading such buses. Considering bus 3 in Table 7, it can be seen that, for the case with DPF = 0.90, the increase in the active demand is 44.03 MW, while for the case with DPF = 0.95 it is 5.22 MW, and for both DPFs, the reactive demands are equal to their initial values, 1.20 MVar. The new loading factors are 0.999, and 0.988, respectively. This confirms that: (1) the loading factors in the DPFA are controllable, and (2) the active and reactive loading rates in the DPFA are flexible in order to adjust and keep the loading factor within the desired range, as mentioned. Considering bus 5 for both DPFs shows that the reactive demands are also loaded for the cases with DPF = 0.90 and DPF = 0.95, showing the capability of the DPFA to adjust the demands to satisfy the desired DPF. Although the DEPSO model is capable of loading the buses which are initially under the no-load condition, the reactive demands are fixed to their initial values which may cause unrealistic results.

Table 8 presents the bus voltages of the 30-bus-M system under the maximum loading condition. As it is clear from this table, the worst voltage profile corresponds to the DEPSO model where all the maximum voltage magnitudes are lower than or equal to 1 p.u. In terms of voltage profiles all the buses have a good voltage stability condition for both DPFs in the DPFA. In addition, the DPFA provides a flexible loading pattern and the best MLP.

In Fig. 4, the DPF of four buses, with initial DPFs lower than 0.90, are depicted, where the demand power factors are initially 0.8944, 0.7071, 0.8423, and 0.7923, for buses 3, 8, 21, and 23, respectively. This figure reveals that although the DPFs of the DEPSO approach have improved for all buses, it still cannot control them. Unlike the DEPSO approach, the other approaches, except the DPFA, show fluctuations, i.e. in some buses the initial DPFs have improved, while in the other buses, they have worsened. However, the DPFA model is the only model whose DPFs always improve and are under control, by providing a flexible loading pattern. Moreover, this figure shows that bus 3 not only satisfies the desired DPFs but also shows much higher DPFs, i.e., the consumers at this bus demand less reactive power than the maximum allowable limit.

3.3. Case 3: IEEE 57-bus system

The IEEE 57-bus system, which represents a simple approximation of the American power system (in the U.S. Midwest) in the early 1960s [39,43], contains 50 load buses, 7 generation units, and 80 transmission lines. This system is mainly used to show the importance of determining an inappropriate DPF. The initial active and reactive loads of this system are 1250.8 MW and 336.4 MVar, respectively.

From Table 4, in this case and unlike the previous cases, heuristic-based approaches, PSO, HPSO, and SCGA, have greater efficiencies in finding MLPs. The SCGA obtains the best result, 1448.63 MW in 148.76 s, and the DLR-2 and the ILF models obtain 1250.80 MW in 0.279 s and 0.096 s, respectively, showing the

Table 8
Bus voltages (p.u.) of the 30-bus-M system at MLP.

Bus	DEPSO [33]	CLF	DLR-1	DLR-2	ILF	DPFA	
						DPF = 0.90	DPF = 0.95
1	1.0	1.05	1.05	1.02641	1.05	1.05	1.05
2	1.0	1.04574	1.04784	1.01727	1.04681	1.04644	1.04667
3	0.97261	1.01977	1.02437	1.00384	0.99321	1.02638	1.02953
4	0.96960	1.01498	1.02224	0.99975	1.00886	1.02677	1.02669
5	0.97364	1.03498	1.0467	1.0162	1.04594	1.03287	1.04348
6	0.96268	1.00375	1.01693	0.99295	1.01203	1.02123	1.01865
7	0.95736	0.99885	1.01648	0.98838	1.01647	1.01696	1.01753
8	0.94999	0.98114	1.00301	0.98073	1.00061	1.0068	1.00151
9	0.97558	1.01632	1.0239	0.99790	1.02081	1.0289	1.02559
10	0.98315	1.02311	1.02803	1.00132	1.02545	1.03297	1.02924
11	0.97539	1.01632	1.0239	0.99703	1.02081	1.0289	1.02559
12	0.98296	1.04446	1.04609	1.00893	1.04897	1.05	1.05
13	1.0	1.1	1.1	1.02979	1.1	1.08684	1.08756
14	0.97331	1.02557	1.02226	0.99997	1.03557	1.04008	1.03944
15	0.97380	1.03028	1.02803	1.0046	1.03407	1.0439	1.04212
16	0.97519	1.02242	1.0207	0.99790	1.03183	1.03523	1.03186
17	0.97536	1.01339	1.01667	0.99480	1.02214	1.02788	1.023
18	0.96300	1.00444	0.99466	0.98889	0.99076	1.02761	1.02463
19	0.96118	0.99571	0.98721	0.98380	0.97024	1.02154	1.01795
20	0.96574	1.00089	0.99314	0.98693	0.96520	1.02355	1.01991
21	0.99266	1.03607	1.04293	1.00969	1.04281	1.04287	1.03665
22	1.0	1.047	1.05276	1.0163	1.05194	1.0503	1.04435
23	1.0	1.05912	1.06111	1.03066	1.06393	1.06394	1.06012
24	0.98684	1.03839	1.04206	1.01379	1.05	1.04701	1.0401
25	0.98781	1.05	1.05	1.01488	1.05	1.05	1.05
26	0.96521	1.01832	0.99657	0.99615	1.03304	1.02992	1.02419
27	1.0	1.07298	1.08165	1.02553	1.05833	1.06854	1.0688
28	0.96445	1.00832	1.02197	0.99532	1.0174	1.02503	1.02324
29	0.97831	1.03674	1.03002	1.00429	1.0184	1.04958	1.04931
30	0.96531	1.01598	1.01676	0.99270	1.01593	1.03869	1.03864

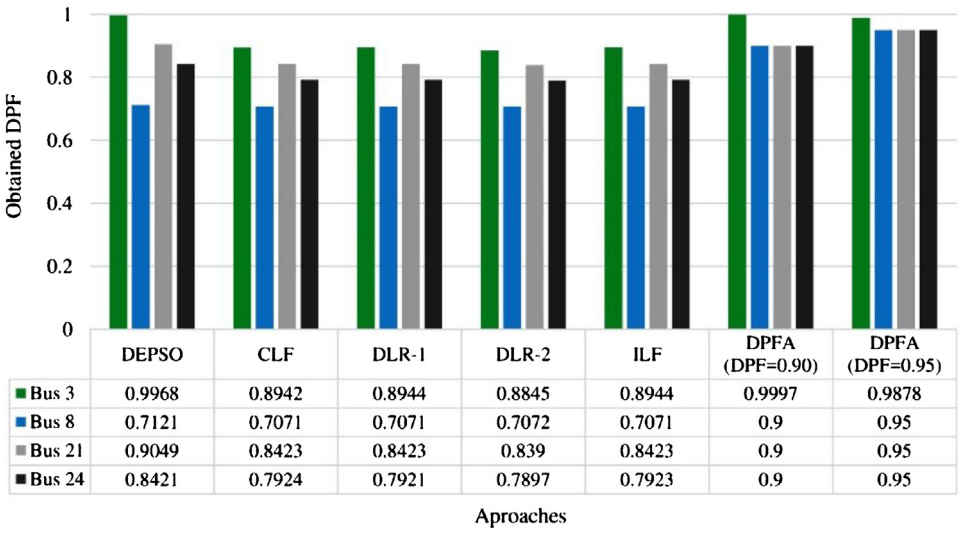

Fig. 4. Demand power factor at four selected buses using different approaches—IEEE 30-bus-M system.

lowest efficiency. The proposed DPFA with DPF = 0.90 shows the greatest efficiency by finding the highest MLP, 1933.62 MW, in the lowest CPU time, 0.093 s. This MLP is 33.48% higher than the MLP of the SCGA and it is 1598.57 times faster. On the other hand, it can be seen that the DPFA with DPF = 0.95 does not converge. This is mainly because of the critical loading condition and configuration of this system which makes it impossible to keep the DPFs of all PQ buses greater than or equal to 0.95.

3.4. Case 4: IEEE 118-bus system

This system contains 64 PQ buses, 54 generation units, and 186 transmission lines [39]. For this system, the initial active and reactive loads are 4242 MW and 1438 MVar, respectively.

From Table 4, the ILF with 9354.91 MW and SCGA with 4739.25 MW shows the best and worst results among the approaches presented, except for the DPFA. The MLP obtained by the DPFA for DPF = 0.90 is 9839.39 MW and for DPF = 0.95 is 9835.24 MW, which are 484.48 MW and 480.33 MW more than the MLP obtained by the ILF model, respectively. Additionally, as seen in Table 5, the proposed DPFA is much faster than the heuristic-based approaches and slightly faster than the ILF model. For the

Table 9
Statistics of the approaches in finding the MLP of different systems.

Systems	Statistics	CLF	DLR-1	DLR-2	ILF	DPFA	
						DPF = 0.90	DPF = 0.95
14-bus, C3	# of variables	114	114	114	121	131	131
	# of constraints	104	104	104	104	113	113
	Evaluation time (s)	0.011	0.001	NC	0.002	0.013	0.014
	# of iterations	13	12	NC	13	14	14
	Total time (s)	0.030	0.037	NC	0.028	0.027	0.035
	TPI (s)	0.00231	0.00308	NC	0.00215	0.00193	0.00250
30-bus	# of variables	236	236	260	253	292	292
	# of constraints	224	224	224	224	248	248
	Evaluation time (s)	0.005	0.012	0.039	0.022	0.019	0.015
	# of iterations	8	11	30	11	16	13
	Total time (s)	0.042	0.048	0.190	0.043	0.060	0.056
	TPI (s)	0.00525	0.00436	0.00633	0.00391	0.00375	0.00431
30-bus-M	# of variables	236	236	260	253	283	283
	# of constraints	224	224	224	224	248	248
	Evaluation time (s)	0.014	0.006	0.033	0.017	0.017	0.015
	# of iterations	11	9	26	12	10	16
	Total time (s)	0.068	0.031	0.177	0.039	0.046	0.054
	TPI (s)	0.00618	0.00344	0.00681	0.00325	0.00460	0.00338
57-bus	# of variables	448	448	498	447	547	547
	# of constraints	434	434	434	434	484	484
	Evaluation time (s)	0.023	0.025	0.057	0.008	0.026	NC
	# of iterations	14	14	24	5	15	NC
	Total time (s)	0.097	0.132	0.279	0.096	0.093	NC
	TPI (s)	0.00693	0.00943	0.01163	0.01920	0.00620	NC
118-bus	# of variables	1088	1088	1152	1141	1215	1215
	# of constraints	980	980	980	980	1044	1044
	Evaluation time (s)	0.354	0.220	NC	0.083	0.138	0.130
	# of iterations	46	27	NC	17	16	15
	Total time (s)	0.947	0.835	NC	0.448	0.312	0.271
	TPI (s)	0.02059	0.03093	NC	0.02635	0.01950	0.01807
2383-bus	# of variables	16,873	16,873	18,929	18,375	20,984	20,984
	# of constraints	16,350	16,350	16,350	16,350	18,406	18,406
	Evaluation time (s)	5.213	5.026	6.151	22.228	2.390	2.646
	# of iterations	42	32	36	179	28	30
	Total time (s)	24.128	24.389	191.711	75.987	6.902	7.424
	TPI (s)	0.57448	0.76216	5.32531	0.42451	0.24650	0.2475

cases with DPF = 0.90 and 0.95, the DPFA only needs 0.312 s and 0.271 s to achieve the optimal solution, respectively, while the other approaches cannot reach such solution and they need more CPU time to converge. In the IEEE 118-bus system, the major shortcoming of the DLR-2 model is revealed, where, as in the IEEE 14-bus system, it is incapable of finding even a bad solution using a commercial solver.

3.5. Case 5: 2383-bus Polish system

The 2383-bus Polish power system with 2056 PQ buses is considered as a very large-scale problem. This system comprises 327 generators, 2896 branches, and 1503 out of 2383 buses are initially loaded and they are spread throughout the network. The initial active and reactive demands for this system are 24,558.38 MW and 8143.92 MVar, respectively. Two buses of this system, 213 and 2164, have initial negative active demands, −2.04 MW and −2 MW, respectively. As mentioned before, these buses imply that there are suppliers and power productions are fixed at their initial values.

It can be seen from Table 4 that the proposed DPFA for both DPFs achieves the best solution. The MLPs of the DPFA with DPF = 0.90 and DPF = 0.95 are 29,142.98 MW and 29,106.85 MW, respectively. These MLPs are 1 GW higher than the MLP of the next best approach, ILF, with 28096.83 MW. As seen in Table 5, the computational efficiency of the DPFA is much higher than in the other approaches. While the ILF model needs 75.987 s to converge to a near- optimal solution, the proposed DPFA only spends 6.902 s for the case with DPF = 0.90, and 7.424 s for the case with DPF = 0.95. This confirms the capability and potential of the proposed model in finding an acceptable MLP.

4. Performance analysis

This section provides detailed information about the number of variables, number of constraints, number of iterations, evaluation time, total time, and the time per iteration (TPI) to analyze the performances of the approaches presented.

Table 9 shows the statistics for commonly used models in literature as well as the proposed DPFA model. As it can be seen from this table, the number of variables and constraints of the proposed model is higher than those of existing models in literature. These variables and constraints correspond to the DPF equations. However, not always do more constraints and variables result in less computational efficiency, this greatly depends on the model and the degree of freedom that this model may provide for a commercial solver. In other words, a solver-friendly model may reach a more precise solution within an acceptable CPU time. A solver-friendly model is a model that is adaptable by using the pre-solving and solving steps of a commercial solver. The pre-solving step aims at reducing the size of the problem and improving the formulation via pre-processing and probing techniques [44], while the solving step mainly focuses on using proper techniques for solving the simplified model resulting from the pre-solving step.

A comparison of the evaluation time of the proposed model with the other approaches shows the superiority of the proposed model in which, when increasing the size of the system, its evaluation

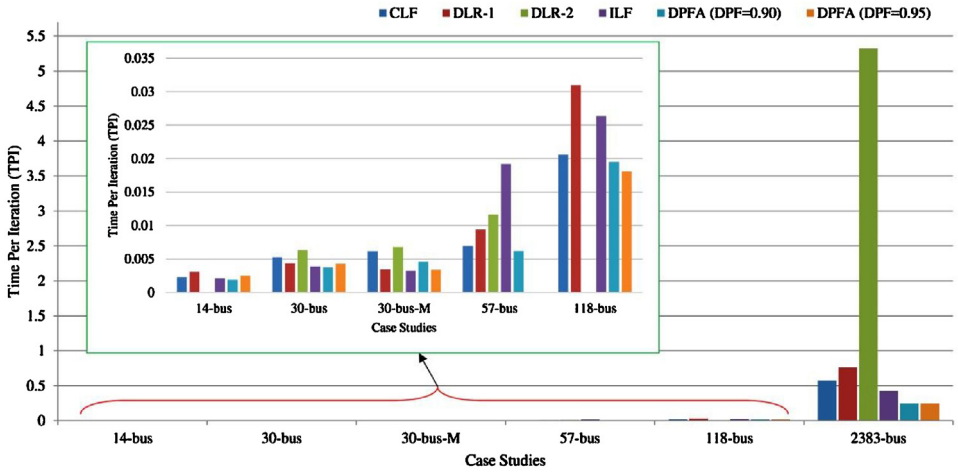

Fig. 5. Time per iteration (TPI) index of different approaches in solving different case studies.

Table 10
The best (green color) and the worst (red color) MLPs and CPU times for each case (for interpretation of the references to color in this table legend, the reader is referred to the web version of this article).

System		CLF	DLR-1	DLR-2	ILF	DPFA
14-bus, C3	MLP		●			●
	Time		▲			▲
30-bus	MLP			●		●
	Time			▲	▲	
30-bus-M	MLP			●		●
	Time			▲	▲	
57-bus	MLP			●	●	●
	Time			▲		▲
118-bus	MLP		●			●
	Time	▲				▲
2383-bus	MLP			●		●
	Time			▲		▲

time is much lower than in the other approaches. The evaluation time contains the evaluation of functions, gradients, and Hessians. Therefore, the lower the evaluation time, the more solver-friendly the model. In order to show the performance of the approaches in the solving step, a time per iteration (TPI) index has been defined as the average time spent at each iteration to find the solution. This index shows the adaptability of the model with the commercial solver KNITRO and is portrayed in Fig. 5. It can be seen from this figure and from the information in Table 9 that, although for small- and medium-scale systems the TPIs do not show significant differences, for a very large-scale system the TPIs of the proposed approach are much better than for the other approaches, with (at least) a 50% improvement for the proposed DPFA model, while the worst results correspond to DLR-2 with a TPI of 5.33 s.

Table 10 shows which approach has the best performance among the presented approaches regarding the solution and CPU times in solving different case studies. As it is evident from this table, the proposed DPFA model always finds the best solution, while the worst solutions correspond to DLR-1 (14-bus, C3, and 118-bus systems) and DLR-2 (30-, modified 30-, 57-, and 2383-bus systems). The CPU times reveal that, except for the 30-bus and 30-bus-M systems, for which the ILF approach shows better computational efficiency, in the other four cases, and most importantly in the very large-scale Polish system, the proposed DPFA model shows higher computational efficiency.

5. Conclusions

The lack of a practical optimal power flow-based model aimed at finding the MLP of a system as the keystone of some planning-, scheduling-, and market-based problems is the main motivation to propose a practical demand power factor-based approach (DPFA). This model is based on practical system operating rules and fills the existing gaps in this area by addressing several drawbacks. In the DPFA, PQ buses without an initial load can be loaded; the demand power factors (DPF) at all buses are controlled, which avoids the consumers from a surcharge; and the active and reactive demands can increase at different rates, which improves the degree of freedom of the system and, therefore, keeps the DPF at the desired level and greatly improves the computational efficiency. Results show that the DPFA does not present the difficulties of heuristic-based approaches, which are population-based, whose results highly depend on the adjustment of parameters and may vary with different trials, and, consequently, their efficiency in facing a different system may also vary. In addition, other models in the literature show fluctuations in finding the solution of differ-

ent systems, e.g. a model may find an optimal solution for some systems but it may not even find a near-optimal solution for other systems. In contrast, the DPFA always overcomes such difficulties finds the best optimal solution as a result of its flexibility. The results show the effectiveness, usefulness, and superiority of the proposed DPFA in finding the MLP of large-scale power systems with a high computational efficiency.

The prospects for the future works are: (1) proposing a stochastic or robust model to consider the imperfect information, and (2) considering the surcharge cost corresponds to the DPF violation in reactive power pricing approaches.

Acknowledgements

The authors would like to gratefully acknowledge the financial support for this research by Fundação de Amparo à Pesquisa do Estado de São Paulo (FAPESP) (Grant Nos. 2014/22828-3, 2016/14319-7), CNPq No. 305371/2012-6, and CAPES.

References

[1] Y.-C. Chang, Multi-objective optimal thyristor controlled series compensator installation strategy for transmission system loadability enhancement, Gener. Transm. Distrib. IET 8 (March (3)) (2014) 552–562.
[2] P. Acharjee, Identification of maximum loadability limit and weak buses using security constraint genetic algorithm, Int. J. Electr. Power Energy Syst. 36 (1) (2012) 40–50.
[3] S.D. Naik, M.K. Khedkar, S.S. Bhat, Effect of line contingency on static voltage stability and maximum loadability in large multi bus power system, Int. J. Electr. Power Energy Syst. 67 (2015) 448–452.
[4] M.R. Mansour, L.F.C. Alberto, R.A. Ramos, Preventive control design for voltage stability considering multiple critical contingencies, IEEE Trans. Power Syst. 31 (March (2)) (2016) 1517–1525.
[5] P. Prakash, D.K. Khatod, Optimal sizing and siting techniques for distributed generation in distribution systems: a review, Renew. Sustain. Energy Rev. 57 (2016) 111–130.
[6] L. Rocha, R. Castro, J.M.F. de Jesus, An improved particle swarm optimization algorithm for optimal placement and sizing of STATCOM, Int. Trans. Electr. Energy Syst. 26 (4) (2016) 825–840.
[7] A.J. Conejo, L.B. Morales, S.J. Kazempour, A.S. Siddiqui, Investment in Electricity Generation and Transmission, Springer International Publishing, 2016.
[8] S. Binato, M.V.F. Pereira, S. Granville, A new Benders decomposition approach to solve power transmission network design problems, IEEE Trans. Power Syst. 16 (May (2)) (2001) 235–240.
[9] N. Alguacil, A.L. Motto, A.J. Conejo, Transmission expansion planning: a mixed-integer LP approach, IEEE Trans. Power Syst. 18 (August (3)) (2003) 1070–1077.
[10] Z. Hu, X. Wang, Efficient computation of maximum loading point by load flow method with optimal multiplier, Power Syst. IEEE Trans. 23 (May (2)) (2008) 804–806.
[11] A. Kazemi, B. Badrzadeh, Modeling and simulation of SVC and TCSC to study their limits on maximum loadability point, Int. J. Electr. Power Energy Syst. 26 (8) (2004) 619–626.
[12] C. Gómez-Quiles, A. Gómez-Expósito, W. Vargas, Computation of maximum loading points via the factored load flow, IEEE Trans. Power Syst. 31 (5) (2016) 4128–4134.
[13] G. Yang, G. Hovland, R. Majumder, Z. Dong, TCSC allocation based on line flow based equations via mixed-integer programming, Power and Energy Society General Meeting—Conversion and Delivery of Electrical Energy in the 21st Century, 2008 IEEE (2008), p. 1.
[14] M. Pourakbari-Kasmaei, M.J. Rider, J.R.S. Mantovani, An unequivocal normalization-based paradigm to solve dynamic economic and emission active-reactive OPF (optimal power flow), Energy 73 (2014) 554–566.
[15] F. Milano, C.A. Canizares, M. Invernizzi, Multiobjective optimization for pricing system security in electricity markets, Power Syst. IEEE Trans. 18 (May (2)) (2003) 596–604.
[16] A.L. Ara, A. Kazemi, S.A.N. Niaki, Multiobjective optimal location of FACTS shunt-series controllers for power system operation planning, IEEE Trans. Power Deliv. 27 (April (2)) (2012) 481–490.
[17] I. El-Samahy, K. Bhattacharya, C. Canizares, M.F. Anjos, J. Pan, A procurement market model for reactive power services considering system security, IEEE Trans. Power Syst. 23 (February (1)) (2008) 137–149.
[18] A.A. EL-Dib, H.K.M. Youssef, M.M. EL-Metwally, Z. Osman, Maximum loadability of power systems using hybrid particle swarm optimization, Electr. Power Syst. Res. 76 (6–7) (2006) 485–492.
[19] M.M.A. Abdelaziz, E.F. El-Saadany, Maximum loadability consideration in droop-controlled islanded microgrids optimal power flow, Electr. Power Syst. Res. 106 (2014) 168–179.
[20] G.D. Irisarri, X. Wang, J. Tong, S. Mokhtari, Maximum loadability of power systems using interior point nonlinear optimization method, Power Syst. IEEE Trans. 12 (February (1)) (1997) 162–172.
[21] T. Van Cutsem, Voltage instability: phenomena, countermeasures, and analysis methods, Proc. IEEE 88 (February (2)) (2000) 208–227.
[22] M. Saravanan, S.M.R. Slochanal, P. Venkatesh, J.P.S. Abraham, Application of particle swarm optimization technique for optimal location of FACTS devices considering cost of installation and system loadability, Electr. Power Syst. Res. 77 (3–4) (2007) 276–283.
[23] I.A. Calle, E.D. Castronuovo, P. Ledesma, Maximum loadability of an isolated system considering steady-state and dynamic constraints, Int. J. Electr. Power Energy Syst. 53 (2013) 774–781.
[24] M.H. Hemmatpour, M. Mohammadian, A.A. Gharaveisi, Simple and efficient method for steady-state voltage stability analysis of islanded microgrids with considering wind turbine generation and frequency deviation, IET Gener. Transm. Distrib. 10 (7) (2016) 1691–1702.
[25] O.O. Obadina, G.J. Berg, Determination of voltage stability limit in multimachine power systems, Power Syst. IEEE Trans. 3 (November (4)) (1988) 1545–1554.
[26] W. Rosehart, C. Canizares, V. Quintana, Costs of voltage security in electricity markets, Power Engineering Society Summer Meeting, 2000. IEEE 4 (2000) 2115–2120.
[27] A.C.Z. de Souza, L.M. Honorio, G.L. Torres, G. Lambert-Torres, Increasing the loadability of power systems through optimal-local-control actions, Power Syst. IEEE Trans. 19 (February (1)) (2004) 188–194.
[28] T. Duong, Y. JianGang, V. Truong, Application of min cut algorithm for optimal location of FACTS devices considering system loadability and cost of installation, Int. J. Electr. Power Energy Syst. 63 (2014) 979–987.
[29] P. Acharjee, S. Mallick, S.S. Thakur, S.P. Ghoshal, Detection of maximum loadability limits and weak buses using Chaotic PSO considering security constraints, Chaos Solitons Fractals 44 (8) (2011) 600–612.
[30] R.J. Avalos, C.A. Canizares, F. Milano, A.J. Conejo, Equivalency of continuation and optimization methods to determine saddle-node and limit-induced bifurcations in power systems, Circuits Syst. I Regul. Pap. IEEE Trans. 56 (January (1)) (2009) 210–223.
[31] R.S. Salgado, A.F. Zeitune, A direct method based on tensor calculation to determine maximum loadability power flow solutions, Electr. Power Syst. Res. 103 (2013) 114–121.
[32] R. Salgado, J. Takashiba, A framework to study QV-constraint exchange points in the maximum loadability analysis, Int. J. Electr. Power Energy Syst. 64 (2015) 347–355.
[33] K. Gnanambal, C.K. Babulal, Maximum loadability limit of power system using hybrid differential evolution with particle swarm optimization, Int. J. Electr. Power Energy Syst. 43 (1) (2012) 150–155.
[34] E.M. Viana, E.J. de Oliveira, N. Martins, J.L.R. Pereira, L.W. de Oliveira, An optimal power flow function to aid restoration studies of long transmission segments, Power Syst. IEEE Trans. 28 (February (1)) (2013) 121–129.
[35] Online, Reactive Support and Control Whitepaper, NERC, 2009.
[36] M. Pourakbari-Kasmaei, M.J. Rider, J.R.S. Mantovani, Multi-area environmentally constrained active-reactive optimal power flow: a short-term tie line planning study, IET Gener. Transm. Distrib. 10 (2) (2016) 299–309.
[37] R. Fourer, D.M. Gay, B.W. Kernighan, AMPL: A Modeling Language for Mathematical Programming, Duxbury Press, 2002.
[38] R. Byrd, J. Nocedal, R. Waltz, Knitro: an integrated package for nonlinear optimization, in: G. Di Pillo, M. Roma (Eds.), Large-Scale Nonlinear Optimization, vol. 83, Springer, US, 2006, pp. 35–59.
[39] Online, Power Systems Test Case, https://www.ee.washington.edu/research/pstca/.
[40] A. Shunmugalatha, S.M.R. Slochanal, Optimum cost of generation for maximum loadability limit of power system using hybrid particle swarm optimization, Int. J. Electr. Power Energy Syst. 30 (8) (2008) 486–490.
[41] A. Shunmugalatha, S.M.R. Slochanal, Maximum loadability limit of a power system using multiagent-based hybrid particle swarm optimization, Electr. Power Compon. Syst. 36 (6) (2008) 575–586.
[42] S. Halder, A. Chakrabarti, Power System Analysis: Operation and Control, PHI Learning, 2010.
[43] B. Gasbaoui, B. Allaoua, Ant colony optimization applied on combinatorial problem for optimal power flow solution, Leonardo J. Sci. 14 (2009) 1–17.
[44] M. Pourakbari-Kasmaei, M.J. Rider, J.R.S. Mantovani, An unambiguous distance-based MIQP model to solve economic dispatch problems with disjoint operating zones, Power Syst. IEEE Trans. 31 (January (1)) (2016) 825–826.